

Approximating electronically excited states with equation-of-motion linear coupled-cluster theory

Jason N. Byrd,^{1, a)} Varun Rishi,¹ Ajith Perera,¹ and Rodney J. Bartlett^{1, 2}

¹⁾ *Quantum Theory Project, University of Florida, Gainesville, FL 32611*

²⁾ *Max-Planck-Institut für Kohlenforschung, Kaiser-Wilhelm-Platz 1, D-45470 Mülheim an der Ruhr, Germany*

A new perturbative approach to canonical equation-of-motion coupled-cluster theory is presented using coupled-cluster perturbation theory. A second-order Møller-Plesset partitioning of the Hamiltonian is used to obtain the well known equation-of-motion many-body perturbation theory (EOM-MBPT(2)) equations and two new equation-of-motion methods based on the linear coupled-cluster doubles (EOM-LCCD) and linear coupled-cluster singles and doubles (EOM-LCCSD) wavefunctions. This is achieved by performing a short-circuiting procedure on the MBPT(2) similarity transformed Hamiltonian. These new methods are benchmarked against very accurate theoretical and experimental spectra from 25 small organic molecules. It is found that the proposed methods have excellent agreement with canonical EOM-CCSD state for state orderings and relative excited state energies as well as acceptable quantitative agreement for absolute excitation energies compared with the best estimate theory and experimental spectra.

I. INTRODUCTION

Optical spectroscopy is an important and ubiquitous tool in modern experimental studies. Improvements over the years in the use of lasers in optical spectroscopy has brought the field to an impressive level of accuracy and precision that is difficult to match using modern theoretical methods. Even so, theory has an important role to play in optical spectroscopy. By assisting in excited state assignments and predicting the density of excited states expected in a given energy range, computational results can be a powerful tool for spectroscopists.

Widespread use of time dependent density functional theory¹ (TD-DFT) for the calculation of excited states will continue for a long time to come due to the attractive low computational scaling inherent to the method. However, reliability and accuracy problems² in TD-DFT keep the theory from replacing the more computationally expensive but highly accurate multireference configuration interaction³ (MRCI) or equation of motion coupled-cluster^{4,5} (EOM-CC) theories. The most commonly used form of EOM-CC theory is the EOM-CCSD variant,⁶ which limits ground and excited state excitations to singles and doubles only. This approximation is qualitatively consistent and approaches quantitative accuracy in many cases where single excitations are dominant. For doubly excited states, perturbative⁷ (EOM-CCSD(T)) or iterative⁸ (EOM-CCSDT-n) triple excitations are required^{9,10} to obtain quantitative agreement with experiment.

The development of approximate excited state methods based on many-body perturbation and coupled-cluster theory has been an active and fruitful endeavour since the emergence of the field.¹¹ Many approaches make use of a mean-field starting reference based on configuration interaction singles¹² and add per-

turbative corrections to that reference.¹³⁻¹⁸ Other approaches use a many-body treatment of propagator theory such as the algebraic-diagrammatic construction^{19,20} (ADC) scheme or by using approximate coupled-cluster linear-response²¹⁻²³ theory with the CCn methods.²⁴ Approximate methods based on equation-of-motion theory can either add a *post hoc* EOM-CC perturbative correction^{7,25,26} for triples or an *a priori* perturbative approximation.²⁷⁻²⁹ We will use perturbation theory here to develop a new perturbative EOM-CC method that also includes infinite-order effects in the ground state wavefunction. The goal will be to provide a consistent and accurate way to obtain excitation energies from either a linear CCD (LCCD) or CCSD (LCCSD) ground state wavefunction. These methods are not intended to be a replacement method for existing fast (EOM-MBPT(2)) or accurate (EOM-CCSD) methods when considering just the calculation of excited states, but to provide a route toward a consistent excited state spectra from a specific ground state wavefunction.

In this work, we will use coupled-cluster perturbation theory³⁰ (CCPT) to derive a general EOM-CCPT framework in Sec. II. The various EOM-CC approximations will then be systematically derived from EOM-CCPT by a choice in the Hamiltonian perturbation partitioning. Numerical results of these approximations compared against very accurate theoretical and experimental spectra are presented in Sec. IV.

II. THEORY

A. Coupled-Cluster Theory

Central to coupled-cluster theory⁴ is the similarity transformation of the electronic Hamiltonian by the exponential wave operator

$$\bar{H} = e^{-\hat{T}} \hat{H} e^{\hat{T}}. \quad (1)$$

^{a)} Electronic mail: byrdja@chem.ufl.edu

The excitation cluster operators (here limited to single and double excitations) are given by

$$\hat{T} = \hat{T}_1 + \hat{T}_2 = \sum_{ai} t_i^a \hat{a}^\dagger \hat{i} + \frac{1}{4} \sum_{abij} t_{ij}^{ab} \hat{a}^\dagger \hat{i} \hat{b}^\dagger \hat{j} \quad (2)$$

and the normal ordered electronic Hamiltonian is

$$\hat{H} = \langle \phi_0 | \hat{H} | \phi_0 \rangle + \sum_{pq} f_q^p \{ p^\dagger q \} + \frac{1}{4} \sum_{pqrs} \bar{v}_{rs}^{pq} \{ p^\dagger q^\dagger sr \} \quad (3)$$

$$= \langle \phi_0 | \hat{H} | \phi_0 \rangle + \hat{F} + \hat{W}. \quad (4)$$

Here f is the one-electron Fock matrix, \bar{v} the antisymmetrized two-electron integrals, $\{\dots\}$ denotes normal ordering of the enclosed operators and the one- (\hat{F}) and two-particle (\hat{W}) are defined appropriately. Throughout we reserve the indices i, j, k, \dots and a, b, c, \dots for occupied and virtual orbitals respectively while the indices p, q, \dots may refer to either occupied or virtual orbitals. Because the Hamiltonian only contains one- and two-particle operators, the Baker-Campbell-Hausdorff expansion of Eq. 1 naturally truncates after four commutators giving

$$\begin{aligned} \bar{H} &= \hat{H} + [\hat{H}, \hat{T}] + \frac{1}{2!} [[\hat{H}, \hat{T}], \hat{T}] + \\ &\frac{1}{3!} [[[[\hat{H}, \hat{T}], \hat{T}], \hat{T}], \hat{T}] + \frac{1}{4!} [[[[[[\hat{H}, \hat{T}], \hat{T}], \hat{T}], \hat{T}], \hat{T}]]. \end{aligned} \quad (5)$$

Starting with an appropriate single-reference mean-field reference, $|\phi_0\rangle$, the coupled-cluster Schrödinger equation is expressed with Eq. 5 as

$$\bar{H}|\phi_0\rangle = E_{CC}|\phi_0\rangle. \quad (6)$$

The CC correlation energy given by projecting on the left by the reference function

$$\langle \phi_0 | \bar{H} | \phi_0 \rangle = E_{CC} \quad (7)$$

while the necessary cluster amplitudes are obtained by solving the equations generated by projecting on the left with the auxiliary space

$$\langle \phi_g | \bar{H} | \phi_0 \rangle = 0 \quad (8)$$

where $\langle \phi_g |$ is the set of g -fold excited determinants

$$\langle \phi_g | = \langle \phi_0 | \hat{i}_1^\dagger \hat{a}_1 \hat{i}_2^\dagger \hat{a}_2 \dots \hat{i}_g^\dagger \hat{a}_g \quad (9)$$

The conventional approach to computing excited states through the equation-of-motion (EOM) method,⁴ which directly computes the k 'th excitation energy (ω_k) relative to the ground state coupled-cluster wavefunction, is also obtained with Eq. 5 as

$$\langle \phi_0 | \hat{L}(k) [\bar{H}, \hat{R}(k)] | \phi_0 \rangle_C = \omega_k. \quad (10)$$

Here ω_k is the k 'th general eigenvalue, and $\hat{R}(k)$ ($\hat{L}(k)$) is the k 'th right (left) general eigenvector solution to the non-Hermitian matrix, \bar{H} . The $\langle \cdot \rangle_C$ denotes that only fully connected contractions are included. These eigenvector solutions are defined as the linear excitation and de-excitation operators (limited again to only singles and doubles)

$$\begin{aligned} \hat{R}(k) &= r_0(k) + \hat{R}_1(k) + \hat{R}_2(k) = \\ &r_0(k) + \sum_{ai} r_i^a(k) \hat{a}^\dagger \hat{i} + \frac{1}{4} \sum_{abij} r_{ij}^{ab}(k) \hat{a}^\dagger \hat{i} \hat{b}^\dagger \hat{j} \end{aligned} \quad (11)$$

$$\hat{L}(k) = \hat{L}_1(k) + \hat{L}_2(k) = \sum_{ai} \ell_a^i(k) \hat{i}^\dagger \hat{a} + \frac{1}{4} \sum_{abij} \ell_{ab}^{ij}(k) \hat{i}^\dagger \hat{a} \hat{j}^\dagger \hat{b}, \quad (12)$$

with the biorthogonalization constraint

$$\langle \phi_0 | \hat{L}(k) \hat{R}(k') | \phi_0 \rangle \equiv \delta_{kk'}. \quad (13)$$

Note that because $\hat{R}(k)$ is an excitation operator, it will commute with the ground state cluster amplitudes

$$[\hat{T}, \hat{R}(k)] = 0. \quad (14)$$

B. Coupled-Cluster Perturbation Theory Similarity Transformed Hamiltonian

As is always possible in Hamiltonian based perturbation theory we can represent the complete Hamiltonian in terms of a zero'th order Hamiltonian \hat{H}_0 and perturbation \hat{V}

$$\hat{H} = \hat{H}_0 + \alpha \hat{V} \quad (15)$$

where $\alpha \rightarrow 1$ is an order parameter used for convenience. Equation 15 can be directly inserted into in any coupled-cluster similarity transformation or energy functional and expanded to the desired order in α . Examples other than the usual form given by Eq. 5 would include the Hermitian^{31,32} ($e^{\hat{T}^\dagger} \hat{H} e^{\hat{T}}$) or unitary³³ ($e^{\hat{T}^\dagger} \hat{H} e^{\hat{T}}$) expansions, but they do not simply terminate without truncation.

To facilitate the decomposition into a reference and perturbation operator, we rearrange the Hamiltonian into particle excitation rank form

$$\hat{H} = \langle 0 | \hat{H} | 0 \rangle + \hat{F}^{[0]} + \hat{F}^{[\pm 1]} + \hat{W}^{[0]} + \hat{W}^{[\pm 1]} + \hat{W}^{[\pm 2]} \quad (16)$$

where the $[n]$ superscript denotes that the operator changes particle rank from right to left by n . From this point the CC perturbation framework used is the same as we have employed in the past.^{18,30,34} Here the exponential wavefunction $e^{\hat{T}}$ is expanded to the appropriate

order in terms of n 'th order cluster operators $\hat{T}^{(n)}$. The computation of these perturbative cluster operators is done order by order using standard perturbation theory.

This is easily illustrated by expanding Eq. 5 using the partitioned Hamiltonian of Eq. 15. The similarity transformed Hamiltonian to arbitrary order in α is given by

$$\begin{aligned} \bar{H}^{(n)} \equiv & \sum_{n'} \left[\left(\hat{H}_0 \delta_{n,n'} + \hat{V} \delta_{n,n'+1} \right), \hat{T}^{(n')} \right] + \frac{1}{2!} \sum_{n'm} \left[\left[\left(\hat{H}_0 \delta_{n,n'+m} + \hat{V} \delta_{n,n'+m+1} \right), \hat{T}^{(m)} \right], \hat{T}^{(n')} \right] + \\ & \frac{1}{3!} \sum_{n'mm'} \left[\left[\left[\left(\hat{H}_0 \delta_{n,n'+m+m'} + \hat{V} \delta_{n,n'+m+m'+1} \right), \hat{T}^{(m)} \right], \hat{T}^{(m')} \right], \hat{T}^{(n')} \right] + \\ & \frac{1}{4!} \sum_{n'mm'm''} \left[\left[\left[\left[\left(\hat{H}_0 \delta_{n,n'+m+m'+m''} + \hat{V} \delta_{n,n'+m+m'+m''+1} \right), \hat{T}^{(m)} \right], \hat{T}^{(m')} \right], \hat{T}^{(m'')} \right], \hat{T}^{(n')} \right]. \end{aligned} \quad (17)$$

Throughout this work we denote the exclusive order in α of an operator with the superscript (n) and we use $\{n\}$ to denote an expansion inclusive of all orders in α up to n . With this notation, the general n 'th order similarity transformed Hamiltonian can be expressed as a compact series

$$\bar{H}^{\{n\}} = \hat{H}_0 + \bar{H}^{(1)} + \dots + \bar{H}^{(n)}. \quad (18)$$

The n 'th order ground state CCPT cluster amplitudes are completely defined from insertion of the exclusive similarity transformed Hamiltonian, Eq. 17, into 8

$$\langle \phi_g | \bar{H}^{(n)} | \phi_0 \rangle = 0. \quad (19)$$

Using these n 'th order ground state amplitudes in Eq. 7 will give the $n+1$ order correlation energy beginning with $n=2$

$$\langle \phi_0 | \bar{H}^{(n+1)} | \phi_0 \rangle = E_{CC}^{(n+1)}. \quad (20)$$

From this the exact coupled-cluster correlation energy, relative to the mean-field energy

$$\Delta E_{CC} = E_{CC} - \langle 0 | \hat{H} | 0 \rangle, \quad (21)$$

is

$$\Delta E_{CC} \simeq \Delta E_{CC}^{(2)} + \Delta E_{CC}^{(3)} + \dots + \Delta E_{CC}^{(n)} \quad (22)$$

or equivalently

$$\Delta E_{CC} \simeq \langle \phi_0 | \bar{H}^{(2)} | \phi_0 \rangle + \dots + \langle \phi_0 | \bar{H}^{(n)} | \phi_0 \rangle \quad (23)$$

$$\equiv \langle \phi_0 | \bar{H}^{\{n\}} | \phi_0 \rangle. \quad (24)$$

To obtain excitation energies relative to the n 'th order energy without perturbatively expanding the \hat{L} and \hat{R} operators, we use the n 'th order *inclusive* similarity transformed Hamiltonian (Eq. 18) in Eq. 10 rather than the *exclusive* Eq. 17, giving

$$\langle \phi_0 | \hat{L}(k) \left[\bar{H}^{\{n\}}, \hat{R}(k) \right] | \phi_0 \rangle = \omega_k. \quad (25)$$

There are many ways to partition the Hamiltonian. We have used the particle rank conserving partitioning of the Hamiltonian,

$$\hat{H}_0 = \langle 0 | \hat{H} | 0 \rangle + \hat{F}^{[0]} + \hat{W}^{[0]} \quad (26)$$

$$\hat{V} = \hat{F}^{[\pm 1]} + \hat{W}^{[\pm 1]} + \hat{W}^{[\pm 2]}, \quad (27)$$

in previous work^{18,30,34} to great success. Alternatively we can also choose the traditional Møller-Plesset (MP) partitioning which we will discuss next.

C. Second-Order Møller-Plesset Partitioning

The standard approach in electronic structure theory is to use generalized many-body perturbation theory (GMBPT),³⁵ based on the Møller-Plesset (MP) partitioning of the Hamiltonian, given by

$$\hat{H}_0 = \hat{F}^{[0]} \quad (28)$$

$$\hat{V} = \hat{F}^{[\pm 1]} + \hat{W}^{[0]} + \hat{W}^{[\pm 1]} + \hat{W}^{[\pm 2]}. \quad (29)$$

Using Eqs. 28 and 29 in Eq. 17, the first two orders of $\bar{H}^{(n)}$ are respectively

$$\bar{H}^{(1)} = \left[\hat{H}_0, \hat{T}^{(1)} \right] + \hat{V} \quad (30)$$

and

$$\bar{H}^{(2)} = \left[\hat{H}_0, \hat{T}^{(2)} \right] + \left[\hat{V}, \hat{T}^{(1)} \right]. \quad (31)$$

Inserting Eq. 30 into Eq. 19 gives the quintessential GMBPT(1) wavefunction

$$\langle \phi_1 | \hat{F}^{[0]} \hat{T}_1^{(1)} + \hat{F}^{[\pm 1]} | \phi_0 \rangle_C = 0 \quad (32)$$

$$\langle \phi_2 | \hat{F}^{[0]} \hat{T}_2^{(1)} + \hat{W}^{[\pm 2]} | \phi_0 \rangle_C = 0 \quad (33)$$

from which

$$E^{(2)} = \langle \phi_0 | \hat{F}^{[-1]} \hat{T}_1^{(1)} + \hat{W}^{[-2]} \hat{T}_2^{(1)} | \phi_0 \rangle_C. \quad (34)$$

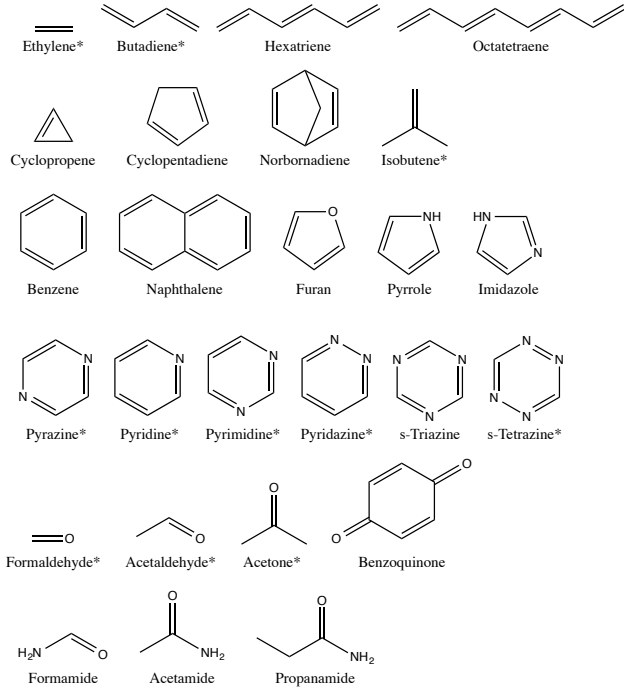


FIG. 1. Member molecules of the Mülheim test set. Names denote with an * are also members of the Yale set, with Acetaldehyde only a member of the Yale set.

The GMBPT(2) wavefunction is

$$\langle \phi_1 | \hat{F}^{[0]} \hat{T}_1^{(2)} + \hat{W}^{[0]} \hat{T}_1^{(1)} + (\hat{F}^{[-1]} + \hat{W}^{[-1]}) \hat{T}_2^{(1)} | \phi_0 \rangle_C = 0 \quad (35)$$

$$\langle \phi_2 | \hat{F}^{[0]} \hat{T}_2^{(2)} + \hat{W}^{[0]} \hat{T}_2^{(1)} + W^{[+1]} \hat{T}_1^{(1)} | \phi_0 \rangle_C = 0. \quad (36)$$

The triples contribution does not contribute to the first- or second-order wavefunction. The inclusive second-order similarity transformed Hamiltonian,

$$\bar{H}^{\{2\}} = \hat{F}^{[0]} + \hat{V} + [\hat{F}^{[0]}, \hat{T}^{(1)}] + [\hat{F}^{[0]}, \hat{T}^{(2)}] + [\hat{V}, \hat{T}^{(1)}], \quad (37)$$

is the GMBPT generalization of previous²⁷⁻²⁹ MBPT approximations to \bar{H} . The spin-orbital equations for the $\bar{H}^{\{2\}}$ matrix elements^{27,28} using Einstein notation are

$$\mathcal{H}_j^i = f_j^i - f_e^i t_j^{e(1)} - \bar{v}_{je}^{im} t_m^{e(1)} + \frac{1}{2} \bar{v}_{ef}^{im} t_{jm}^{ef(1)}, \quad (38)$$

$$\mathcal{H}_b^a = f_b^a + f_b^m t_a^{m(1)} + \bar{v}_{be}^{am} t_m^{e(1)} + \frac{1}{2} \bar{v}_{be}^{mn} t_{mn}^{ae(1)}, \quad (39)$$

$$\mathcal{H}_a^i = f_a^i + \bar{v}_{ae}^{im} t_m^{e(1)}, \quad (40)$$

$$\mathcal{H}_i^a = 0, \quad (41)$$

$$\mathcal{H}_{cd}^{ab} = \bar{v}_{cd}^{ab} + \bar{v}_{cd}^{am} t_m^{b(1)} + \frac{1}{2} \bar{v}_{cd}^{mn} t_{mn}^{ab(1)}, \quad (42)$$

$$\mathcal{H}_{kl}^{ij} = \bar{v}_{kl}^{ij} + \bar{v}_{ke}^{ij} t_\ell^{e(1)} + \frac{1}{2} \bar{v}_{ef}^{ij} t_{kl}^{ef(1)}, \quad (43)$$

$$\mathcal{H}_{bj}^{ia} = \bar{v}_{bj}^{ia} - \bar{v}_{bj}^{mi} t_m^{a(1)} + \bar{v}_{be}^{ia} t_j^{e(1)} + P(ij)P(ab) \bar{v}_{eb}^{mi} t_{mj}^{ae(1)}, \quad (44)$$

$$\mathcal{H}_{ka}^{ij} = \bar{v}_{ka}^{ij} - \bar{v}_{ea}^{ij} t_k^{e(1)}, \quad (45)$$

$$\mathcal{H}_{bc}^{ai} = \bar{v}_{bc}^{ai} + \bar{v}_{bc}^{mi} t_m^{a(1)}, \quad (46)$$

$$\mathcal{H}_{jk}^{ia} = \bar{v}_{jk}^{ia} + \bar{v}_{jk}^{im} t_m^{a(1)} - \bar{v}_{je}^{ia} t_k^{e(1)} + f_e^i t_{jk}^{ea(1)} + \frac{1}{2} \bar{v}_{ef}^{ia} t_{jk}^{ef(1)} - P(jk) \bar{v}_{je}^{im} t_{mk}^{ea(1)}, \quad (47)$$

$$\mathcal{H}_{ci}^{ab} = \bar{v}_{ci}^{ab} - \bar{v}_{ce}^{ab} t_i^{e(1)} + \bar{v}_{ci}^{am} t_m^{b(1)} - \frac{1}{2} \bar{v}_{ci}^{mn} t_{mn}^{ab(1)} + P(ab) \bar{v}_{ce}^{am} t_{mi}^{eb(1)}, \quad (48)$$

$$\mathcal{H}_{ab}^{ij} = \bar{v}_{ab}^{ij}, \quad (49)$$

$$\mathcal{H}_{ij}^{ab} = 0, \quad (50)$$

$$\mathcal{H}_{cdi}^{ajb} = \bar{v}_{cd}^{mj} t_{mi}^{ab(1)}, \quad (51)$$

$$\mathcal{H}_{kbl}^{ija} = -\bar{v}_{be}^{ij} t_{kl}^{ea(1)}, \quad (52)$$

$$\mathcal{H}_{cjk}^{iab} = P(ab) \bar{v}_{ce}^{ia} t_{ij}^{eb(1)} - P(ij) \bar{v}_{cj}^{im} t_{mk}^{ab(1)}, \quad (53)$$

where $P(pq)$ is the anti-permutation operator

$$P(pq)g(pq\dots rs) = g(pq\dots rs) - g(pq\dots sr). \quad (54)$$

The difference between GMBPT and MP theory occurs when f_i^a , f_j^i and $f_b^a \neq 0$ as they would be for canonical HF orbitals. The first introduces a first-order singles wavefunction (Eq. 32), while the second and third terms have to be summed to all order as in coupled-cluster theory or better transformed away by a semi-canonical occupied-occupied and virtual-virtual rotation. The first-order t amplitudes used in Eqs. 38-53 are obtained from Eq. 32 and Eq. 33. Second-order amplitude contributions are limited in this case to \mathcal{H}_i^a and \mathcal{H}_{ij}^{ab} because in the GMBPT partitioning $\hat{F}^{[0]}T^{(2)}$ can only give particle excitation matrix elements. Because these matrix elements are by definition zero (Eq. 8) there are no actual contributions from the second-order amplitudes to the excited state spectrum.

D. Inclusive Second-Order Møller-Plesset Partitioning

The EOM-MBPT(2) approach theoretically suffers from the fact that the starting wavefunction is strictly a single shot perturbation calculation, while the diagonalization of \bar{H} introduces infinite-order contributions to the excitation wavefunction. This can be overcome, while using the GMBPT partitioning, by short-circuiting the

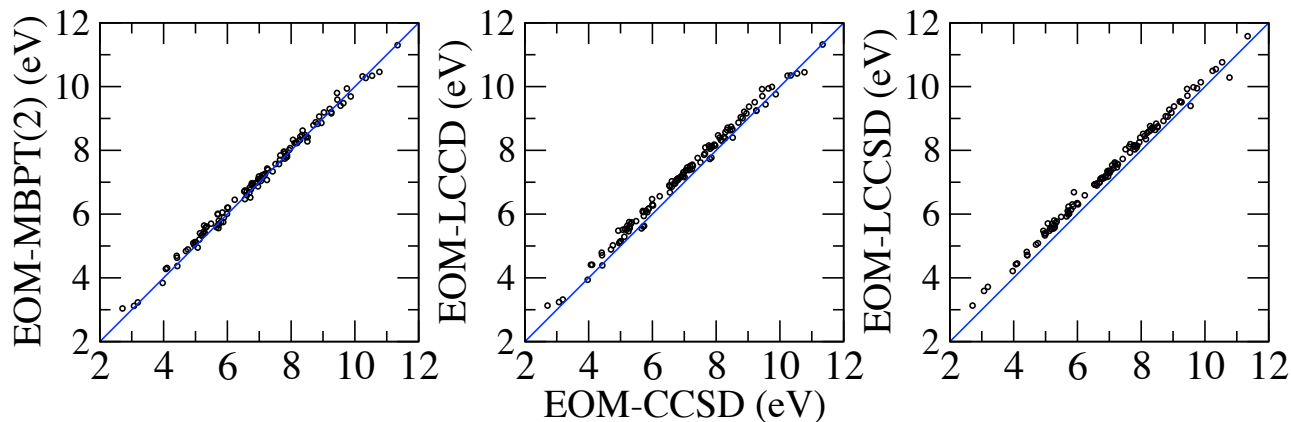


FIG. 2. Comparison against the Mülheim data set EOM-CCSD values.

order-by-order amplitude computation to instead solve

$$\langle \phi_g | \bar{H}^{\{2\}} | \phi_0 \rangle = 0. \quad (55)$$

Here we combine the first- and second-order amplitude equations to obtain

$$\langle \phi_1 | \hat{F}^{[0]} \hat{T}_1^{(1\infty)} + \hat{W}^{[0]} \hat{T}_1^{(1\infty)} + \hat{F}^{[-1]} \hat{T}_2^{(1\infty)} + \hat{W}^{[-1]} \hat{T}_2^{(1\infty)} + F^{[+1]} | \phi_0 \rangle_C = 0 \quad (56)$$

$$\langle \phi_2 | \hat{F}^{[0]} \hat{T}_2^{(1\infty)} + \hat{W}^{[0]} \hat{T}_2^{(1\infty)} + \hat{W}^{[+1]} \hat{T}_1^{(1\infty)} + \hat{W}^{[+2]} | \phi_0 \rangle_C = 0. \quad (57)$$

Equations 56 and 57 are incidentally the linearized CCSD amplitude equations (LCCSD). If the singles contributions in Eq. 56 are removed, the resulting reference wavefunction is then simply linearized CCD (LCCD).³⁶ This is a convenient approximation as it requires no new terms in the similarity transformed Hamiltonian, while introducing infinite-order character to the reference wavefunction.

III. ELECTRONIC STRUCTURE CALCULATIONS

To assess both the quality and general behavior of these EOM approximations when computing vertical excitation energies, we employ two established sets of gas phase molecules (see Figure 1): the set of 24 organic molecules from Schreiber *et al.*^{37–39} (referred to hereafter as the Mülheim set) and the set of 11 organic molecules from Caricato *et al.*^{2,40} (referred to here as the Yale set). This Mülheim set contains 121 reference single excitation energies³⁷ which use molecular geometries obtained with an MP2/6-31G* optimization in which the first row 1s atomic orbitals are dropped. The extent and balanced nature of the Mülheim set readily lends itself to obtaining statistics between different theoretical methods. To

State	MBPT(2)	LCCD	LCCSD	CCSD	Exp.
ethylene					
B_{3u}	7.15	7.43	7.45	7.28	7.11
B_{1u}	7.76	8.13	8.18	7.97	7.65
B_{1g}	7.79	8.08	8.10	7.97	7.80
B_{2g}	7.84	8.12	8.14	7.93	7.90
A_g	8.19	8.46	8.48	8.31	8.28
B_{3u}	8.64	8.92	8.94	8.77	8.62
B_{3u}	8.93	9.20	9.22	9.05	8.90
B_{3u}	9.05	9.33	9.35	9.17	9.08
B_{1g}	9.19	9.46	9.49	9.34	9.20
B_{1u}	9.18	9.47	9.50	9.32	9.33
B_{3u}	9.84	10.11	10.13	9.96	9.51
isobutene					
B_1	6.29	6.54	6.56	6.38	6.17
A_1	6.81	7.06	7.10	6.91	6.70
trans-1,3-butadiene					
B_u	6.12	6.54	6.63	6.29	5.91
B_g	6.17	6.47	6.49	6.24	6.22
A_u	6.47	6.79	6.80	6.55	6.66
B_u	7.06	7.39	7.43	7.16	7.07
B_g	7.28	7.59	7.60	7.36	7.36
A_g	7.54	7.85	7.85	7.61	7.62
B_u	8.08	8.39	8.40	8.15	8.00
MAD	0.09	0.31	0.34	0.14	
RMS	0.12	0.34	0.37	0.19	
MD	0.33	0.63	0.72	0.45	

TABLE I. Excitation energies for a few small alkene molecules computed with the d-aug-cc-pVDZ basis using MP2/6-311+G** geometries. Units are in electron volts (eV), experimental references can be found in Ref. 2.

compare the approximate EOM-CC methods proposed here, we take our best theoretical reference to be EOM-CCSDT-3,⁴¹ which is known to give both accurate results and is a systematic EOM-CC type theory which will

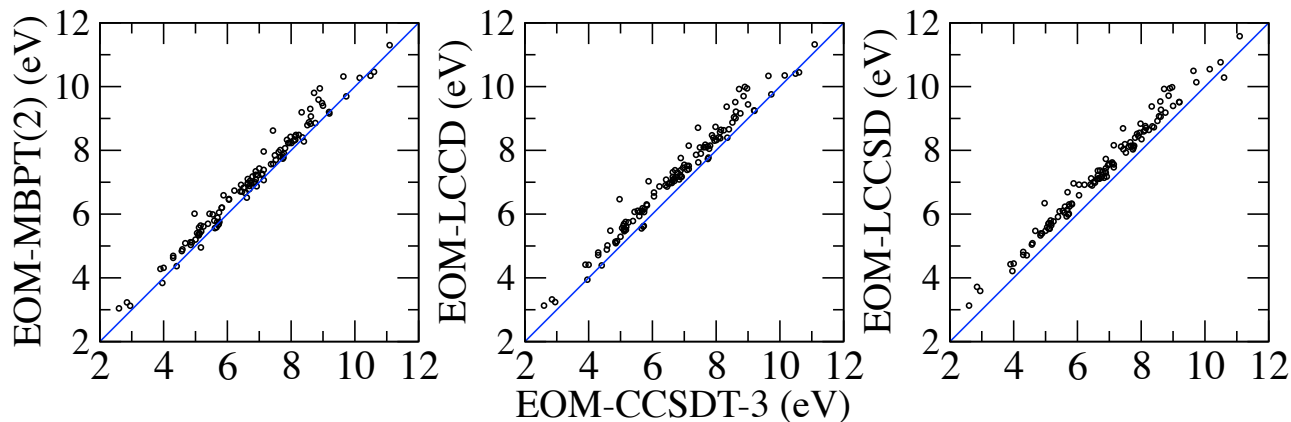


FIG. 3. Comparison against the Mülheim data set EOM-CCSDT-3 values.

provide a balanced comparison. The Yale set choice in molecules is a subset of the Mülheim set with the simple addition of acetaldehyde, but with a different selection in excitation energies (69 in all) whose reference values are taken from gas phase experiments (the experiment literature references can be found in Ref. 2). This comparison to experiment provides a different and valuable perspective with which to augment theory vs. theory examinations. Geometries for the Yale set are obtained from an MP2/6-311+G** optimization.

Calculations using the Mülheim set typically³⁷ use the TZVP basis set ($3s1p$ on hydrogen $5s3p1d$ on first row atoms) from Schäfer *et al.*⁴² This is a light weight basis set that allows the use of many different kinds of computational methods with only a modest cost in overall accuracy.³⁹ While perfectly acceptable when comparing different methods to each other, this basis is not accurate enough to compare with experimental results. This is especially true when calculating Rydberg states, where the inclusion of many diffuse functions is key.^{43,44} When computing the excitation energies for the Yale set, we use the doubly diffuse function augmented Dunning basis,^{45,46} d-aug-cc-pVDZ ($4s3p$ on hydrogen and $5s4p3d$ on first row atoms). This basis is comparable to the 6-311(3+,3+)G** basis used by Caricato *et al.* in their calculations^{2,40,47} with almost no gain in including a third set of diffuse functions.⁴⁸

All of the reported electronic structure results were obtained using the serial ACESII⁴⁹ and parallel Aces4⁵⁰ *ab initio* quantum chemistry packages. Calculations were performed on the University of Florida HiPerGator high performance cluster. Throughout this paper we use RMS to mean "root mean square," MAD to mean "mean average absolute deviation," and MD to mean "absolute maximum deviation."

State	MBPT(2)	LCCD	LCCSD	CCSD	Exp.
acetaldehyde					
A''	4.19	4.28	4.57	4.32	4.28
A'	6.64	6.68	6.94	6.78	6.82
A'	7.32	7.59	7.61	7.67	7.46
A'	7.56	7.37	7.82	7.46	7.75
A'	8.24	8.27	8.51	8.36	8.43
A'	8.27	8.31	8.54	8.39	8.69
acetone					
A_2	4.38	4.44	4.75	4.48	4.43
B_2	6.25	6.29	6.54	6.37	6.36
A_2	7.17	7.19	7.44	7.27	7.36
A_1	7.26	7.29	7.55	7.37	7.41
B_2	7.25	7.27	7.51	7.35	7.49
A_1	7.88	7.90	8.15	7.98	7.80
B_2	7.65	7.68	7.93	7.76	8.09
B_1	7.95	7.98	8.22	8.06	8.17
formaldehyde					
A_2	3.82	3.96	4.23	3.99	4.00
B_2	6.87	6.93	7.17	7.03	7.08
B_2	7.70	7.75	7.96	7.83	7.97
A_1	7.83	7.87	8.10	7.97	8.14
A_2	8.06	8.09	8.32	8.19	8.37
B_2	8.77	8.82	9.05	8.91	8.88
B_1	9.10	9.14	9.05	9.23	9.00
A_2	9.20	9.24	9.45	9.32	9.22
B_2	9.03	9.07	9.29	9.16	9.26
A_1	9.07	9.12	9.35	9.20	9.58
B_2	9.07	9.10	9.32	9.19	9.63
MAD	0.22	0.18	0.14	0.13	
RMS	0.26	0.23	0.17	0.18	
MD	0.56	0.53	0.35	0.44	

TABLE II. Excitation energies for a few small carbonyl molecules computed with the d-aug-cc-pVDZ basis using MP2/6-311+G** geometries. Units are in electron volts (eV), experimental references can be found in Ref. 2.

IV. NUMERICAL RESULTS AND DISCUSSION

A. EOM-MBPT(2)

Developed two decades ago for canonical HF²⁷ EOM-MBPT(2) is a well established perturbation method which has been largely ignored by the community in favor of other approximations such as CC2²⁴ or ADC(2).¹⁹ The EOM-MBPT(2) method remains relevant because of the non-iterative $O(n^5)$ computational cost of the ground-state wavefunction and the general accuracy of MBPT(2). It is also reasonably accurate for equilibrium vertical excitation energies. This accuracy, within the Mülheim test set, is illustrated in the correlation figures 2(a), 3(a) and Table IV. Compared to the standard EOM-CCSD method, EOM-MBPT(2) has an average deviation of 0.13 eV while comparison with EOM-CCSDT-3 gives an average deviation of 0.31 eV respectively, consistent with the known ~ 0.2 eV triples correction to EOM-CCSD.

The EOM-MBPT(2) approximation and its Löwdin partitioned variant^{29,51} was recently benchmarked (using the 6-311(3+,3+)G** basis set) against EOM-CCSD and experiment using the Yale test set by Goings *et al.*⁴⁷ Our computed EOM-MBPT(2)/d-aug-cc-pVDZ values, presented in Tables I, II and III, yield nearly identical results with minor differences due to the alternative basis set choice. The EOM-MBPT(2) method is completely satisfactory when compared to experimental Rydberg states (such as with the alkenes and carbonyl's), but is much less reliable for the $n \rightarrow \pi^*$ and $\pi \rightarrow \pi^*$ heterocycle valence states. The comparative difficulty in describing valence states is a limitation of EOM theory in general which is only satisfactorily overcome in CC theory by using methods that include triples or other methods such as similarity transformed equation-of-motion coupled-cluster theory⁵²⁻⁵⁵ (STEOM-CC).

B. Linear EOM-CC

By employing Eqs. 56 and 57 to compute the amplitudes used in the second-order similarity transformed Hamiltonian $\bar{H}^{\{2\}}$ (Eq. 37), we now have an equation-of-motion theory completely consistent with with the LCCD (LCCSD) wavefunction that only includes terms in the similarity transformed Hamiltonian up to α^2 while ensuring

$$\langle \phi_g | \bar{H} | \phi_0 \rangle = 0. \quad (58)$$

These linear EOM methods have the same iterative $O(n^6)$ computational scaling as canonical EOM-CCSD. However, with the removal of the quadratic amplitude intermediates, the computational overhead and I/O demands are significantly reduced. Benchmark data from the Mülheim set shows a systematic overestimate of exci-

State	MBPT(2)	LCCD	LCCSD	CCSD	Exp.
pyrazine					
B_{3u}	4.52	4.63	4.63	4.33	3.83
B_{2u}	5.36	5.51	5.50	5.10	4.81
B_{2g}	6.17	6.26	6.29	6.01	5.46
B_{1g}	7.14	7.35	7.34	7.07	6.10
B_{1u}	7.04	7.28	7.33	6.95	6.51
pyridazine					
B_1	4.03	4.32	4.36	4.03	3.60
A_1	5.33	5.33	5.75	5.33	5.00
A_2	4.63	4.63	4.96	4.63	5.30
B_1	6.62	6.62	6.93	6.62	6.00
B_2	6.26	6.26	6.43	6.26	6.50
pyridine					
B_1	5.28	5.38	5.46	5.17	4.59
B_2	5.41	5.57	5.61	5.23	4.99
A_2	5.64	5.80	5.92	5.60	5.43
A_1	6.76	6.86	6.92	6.69	6.38
pyrimidine					
B_1	4.74	4.81	4.97	4.63	3.85
A_2	5.07	5.18	5.38	5.03	4.62
B_2	5.66	5.77	5.89	5.47	5.12
A_2	6.26	6.35	6.51	6.18	5.52
B_1	6.53	6.66	6.83	6.50	5.90
A_1	7.02	7.17	7.37	6.96	6.70
s-tetrazine					
B_{3u}	2.97	3.08	3.07	2.67	2.25
A_u	4.16	4.30	4.32	3.98	3.40
A_u	6.00	6.13	6.11	5.72	5.00
B_{3u}	7.11	7.25	7.27	6.95	6.34
MAD	0.60	0.72	0.78	0.49	
RMS	0.64	0.76	0.82	0.53	
MD	1.04	1.25	1.24	0.97	

TABLE III. Excitation energies for a number of single ring azabenzenes computed with the d-aug-cc-pVDZ basis using MP2/6-311+G** geometries. Units are in electron volts (eV), experimental references can be found in Ref. 2.

tation energies for both EOM-LCCD and EOM-LCCSD, with average deviations relative to EOM-CCSD of 0.25 and 0.35 eV respectively (see the correlation figures 2, 3 and Table IV). The comparison of the linear EOM methods against EOM-CCSDT-3 is less satisfactory with a MAD of 0.45 and 0.56 eV for EOM-LCCD and EOM-LCCSD respectively.

However, these methods are not without merit should the ground state wavefunction need to be computed with LCCD or LCCSD. This is an important concern for weakly interacting systems or transition states where an MBPT(2) wavefunction is a poor approximation. With an acceptable standard deviation of 0.11 and 0.10 eV

	MBPT(2)	LCCD	LCCSD
relative to EOM-CCSD			
MAD	0.13	0.25	0.35
RMS	0.15	0.28	0.36
MD	0.37	0.55	0.80
relative to EOM-CCSDT-3			
MAD	0.31	0.45	0.56
RMS	0.38	0.53	0.60
MD	1.19	1.49	1.37

TABLE IV. Excitation energy comparison statistics for the Mülheim test set. Units are in electron volts (eV), EOM-CCSD and EOM-CCSDT-3 reference values were taken from Sous *et al.*⁵⁵

3

compared to EOM-CCSD, the excitation energies and relative state orderings obtained with the linear EOM methods are reliably consistent compared to canonical EOM-CCSD. This is further illustrated in Tables I, II and III where the systematic and consistent overestimation of the excitation energies is balanced by a nearly exact agreement in state ordering *and* relative state energy differences (a MAD of 0.04, 0.04 and 0.05 eV for EOM-MBPT(2), LCCD and LCCSD respectively). For approximate methods, getting these relative properties correct is just as useful as quantitatively accurate excitation energies.

V. CONCLUSIONS

We have expanded the coupled-cluster similarity transformed Hamiltonian using general coupled-cluster perturbation theory to obtain the arbitrary order coupled-cluster perturbation theory effective Hamiltonian given by Eq. 17. The inclusive (the sum of all orders 0 to n) form of the Hamiltonian is inserted into the standard electronic-excitation equation-of-motion theory to give the completely general EOM-CCPT (Eq. 25). The result is a way of using the standard equation-of-motion theory to directly compute excitation energies that are consistent with a given CCPT ground state wavefunction.

By choosing the generalized many-body perturbation theory partitioning of the Hamiltonian, we re-derive the well known EOM-MBPT(2)²⁹ (EOM-CCSD(2)²⁷) equations. An alternative source of amplitudes is obtained by short-circuiting the inclusive $\langle \phi_g | \bar{H}^{\{2\}} | \phi_0 \rangle$ set of equations. The resulting infinite-order amplitudes correspond to the linear CCSD (and CCD in the case of single excitations being neglected) expansion, and their use in the inclusive similarity transformed Hamiltonian in place of the standard MBPT(2) amplitudes provides an equation-of-motion method perturbatively consistent with a LCCD and LCCSD reference wavefunction.

These approximate equation-of-motion methods are

benchmarked by employing the Mülheim³⁷⁻³⁹ and Yale^{2,40} small organic molecule data sets. We use the diverse Mülheim test set to benchmark our new methods against the canonical EOM-CCSD and EOM-CCSDT-3 methods, while the Yale test set is employed in benchmarking against experimental spectra. Our methods are found to consistently over estimate excitation energies, relative to EOM-CCSD and EOM-CCSDT-3 by ~ 0.25 and ~ 0.5 eV respectively. The precise statistics and correlation plots can be found in Table IV and Figures 2 and 3. This systematic overestimation compared to the complete EOM-CCSD suggests that the similarity transformed Hamiltonian (and thus the excited state spectrum) based on the linear CC wavefunction is over-approximated compared to the ground-state description leading to an increased separation. The very good ~ 0.1 eV standard deviation compared with EOM-CCSD suggests that the predicted relative spectra will be much more accurate than the absolute excitation energies. This is supported by studying the benchmark values from the Yale set given in Tables I, II and III where the presented approximate EOM methods obtain relative state orderings and energies to within ~ 0.04 eV of canonical EOM-CCSD.

VI. ACKNOWLEDGMENTS

The authors acknowledge support from the U.S. Air Force Office of Scientific Research grant FA 9550-11-1-0065 and the U.S. Army Research Office DURIP grant W911-12-1-0365 which funded access to the University of Florida Research Computing HiPerGator high performance cluster.

REFERENCES

- ¹A. Dreuw and M. Head-Gordon, Chem. Rev. **105**, 4009 (2005).
- ²M. Caricato, G. W. Trucks, M. J. Frisch, and K. B. Wiberg, J. Chem. Theory Comput. **6**, 370 (2010).
- ³P. G. Szalay, T. Mller, G. Gidofalvi, and H. Lischka, Chem. Rev. **112**, 108 (2012).
- ⁴R. Bartlett and M. Musiał, Rev. Mod. Phys. **79**, 291 (2007).
- ⁵K. Sneskov and O. Christiansen, WIREs: Comput. Mol. Sci. **2**, 566 (2011).
- ⁶J. F. Stanton and R. J. Bartlett, J. Chem. Phys. **98**, 7029 (1993).
- ⁷T. J. Watson Jr., V. F. Lotrich, P. G. Szalay, A. Perera, and R. J. Bartlett, J. Phys. Chem. A **117**, 2569 (2013).
- ⁸J. D. Watts and R. J. Bartlett, J. Chem. Phys. **101**, 3073 (1994).
- ⁹J. E. Del Bene, J. D. Watts, and R. J. Bartlett, J. Chem. Phys. **106**, 6051 (1997).
- ¹⁰J. D. Watts and R. J. Bartlett, Spectrochim. Acta, Part A **55**, 495 (1999).

- ¹¹J. Paldus, J. Čížek, M. Saute, and A. Laforgue, Phys. Rev. A **17**, 805 (1978).
- ¹²J. Foresman, M. Head-Gordon, and J. Pople, J. Phys. Chem. **96**, 135 (1992).
- ¹³M. Head-Gordon, R. J. Rico, M. Oumi, and T. J. Lee, Chem. Phys. Lett. **219**, 21 (1994).
- ¹⁴S. Hirata, J. Chem. Phys. **122**, 094105 (2005).
- ¹⁵X. Liu, Q. Ou, E. Alguire, and J. E. Subotnik, J. Chem. Phys. **138**, 221105 (2013).
- ¹⁶X. Liu and J. E. Subotnik, J. Chem. Theory Comput. **10**, 1004 (2014).
- ¹⁷X. Liu and J. E. Subotnik, J. Chem. Theory Comput. **10**, 1835 (2014).
- ¹⁸J. N. Byrd, V. F. Lotrich, and R. J. Bartlett, J. Chem. Phys. **140**, 234108 (2014).
- ¹⁹J. Schirmer, Phys. Rev. A **26**, 23952416 (1982).
- ²⁰A. B. Trofimov, I. L. Krivdina, J. Weller, and J. Schirmer, Chem. Phys. **329**, 1 (2006).
- ²¹H. J. Monkhorst, Int. J. Quant. Chem. Symp. **11**, 421 (1977).
- ²²H. Sekino and R. J. Bartlett, Int. J. Quantum Chem. **18**, 255 (1984).
- ²³H. Koch and P. Jørgensen, J. Chem. Phys. **93**, 3333 (1990).
- ²⁴O. Christiansen, H. Koch, and P. Jørgensen, Chem. Phys. Lett. **243**, 409 (1995).
- ²⁵S. Hirata, M. Nooijen, I. Grabowski, and R. J. Bartlett, J. Chem. Phys. **114**, 3919 (2001).
- ²⁶S. Hirata, M. Nooijen, I. Grabowski, and R. J. Bartlett, J. Chem. Phys. **115**, 3967 (2001).
- ²⁷J. Stanton, J. F. and Gauss, J. Chem. Phys. **103**, 1064 (1995).
- ²⁸M. Nooijen and J. G. Snijders, J. Chem. Phys. **102**, 1681 (1995).
- ²⁹S. R. Gwaltney, M. Nooijen, and R. J. Bartlett, Chem. Phys. Lett. **248**, 189 (1996).
- ³⁰R. J. Bartlett, M. Musial, V. F. Lotrich, and T. Kus, in *Recent Progress in Coupled-Cluster Methods*, Vol. 11, edited by P. Carsky, J. Paldus, and J. Pittner (Springer, Dordrecht, 2010) Chap. 1, pp. 1–34.
- ³¹J. Paldus, J. Čížek, and I. Shavitt, Phys. Rev. A **5**, 50 (1972).
- ³²R. J. Bartlett and J. Noga, Chem. Phys. Lett. **150**, 29 (1988).
- ³³R. J. Bartlett, S. A. Kucharski, and J. Noga, Chem. Phys. Lett. **155**, 133 (1989).
- ³⁴J. N. Byrd, N. Jindal, R. W. Molt, Jr., R. J. Bartlett, B. A. Sanders, and V. F. Lotrich, Mol. Phys. **113**, 1 (2015).
- ³⁵I. Shavitt and R. J. Bartlett, *Many-Body Methods in Chemistry and Physics* (Cambridge, New York, 2009).
- ³⁶A. G. Taube and R. J. Bartlett, J. Chem. Phys. **130**, 144112 (2009).
- ³⁷M. Schreiber, M. R. Silva-Junior, S. P. A. Sauer, and W. Thiel, J. Chem. Phys. **128**, 134110 (2008).
- ³⁸S. P. A. Sauer, M. Schreiber, M. R. Silva-Junior, and W. Thiel, J. Chem. Theory Comput. **5**, 555 (2009).
- ³⁹M. R. M. Silva-Junior, M. M. Schreiber, S. P. A. S. Sauer, and W. W. Thiel, J. Chem. Phys. **133**, 174318 (2010).
- ⁴⁰M. Caricato, G. W. Trucks, M. J. Frisch, and K. B. Wiberg, J. Chem. Theory Comput. **7**, 456 (2011).
- ⁴¹Partial inclusion of triples⁵⁶ which has all possible \hat{T}_1 and \hat{T}_2 to \hat{T}_3 with $O(n^7)$ scaling, but neglects the $\hat{T}_3 \rightarrow \hat{T}_3$ contributions that would introduce an $O(n^8)$ step.
- ⁴²A. Schäfer, H. Horn, and R. Ahlrichs, J. Chem. Phys. **97**, 2571 (1992).
- ⁴³S. R. Gwaltney and R. J. Bartlett, Chem. Phys. Lett. **241**, 26 (1995).
- ⁴⁴K. B. Wiberg, A. E. de Oliveira, and G. Trucks, J. Phys. Chem. A **106**, 4192 (2002).
- ⁴⁵T. Dunning Jr, J. Chem. Phys. **90**, 1007 (1989).
- ⁴⁶R. Kendall, T. Dunning Jr, and R. Harrison, J. Chem. Phys. **96**, 6796 (1992).
- ⁴⁷J. J. Goings, M. Caricato, M. J. Frisch, and X. Li, J. Chem. Phys. **141**, 16411610 (2014).
- ⁴⁸Where the d-aug-cc-pVDZ basis is clearly not as accurate as the 6-311(3+,3+)G** basis is in the case of the highest considered excited state of ethylene and formaldehyde.
- ⁴⁹J. F. Stanton, J. Gauss, S. A. Perera, A. Yau, J. D. Watts, M. Nooijen, N. Oliphant, P. G. Szalay, W. J. Lauderdale, S. R. Gwaltney, S. Beck, A. Balková, D. E. Bernholdt, K.-K. Baeck, P. Rozyczko, H. Sekino, C. Huber, J. Pittner, and R. J. Bartlett, “ACESII is a product of the quantum theory project, university of florida,” Integral packages included are VMOL (Almölf, J and Taylor, P. R.) VPROPS (Taylor, P. R.) and ABACUS (Helgaker, T. and Jensen, H. J. Aa. and Jørgensen P. and Olsen J. and Taylor P. R.).
- ⁵⁰B. A. Sanders, N. Jindal, J. N. Byrd, V. F. Lotrich, D. Lyakh, N. Flocke, A. Perera, and R. J. Bartlett, “Aces4 pre-alpha release,” <https://github.com/UFPParLab>.
- ⁵¹P.-O. Löwdin, J. Mol. Spectrosc. **10**, 12 (1963).
- ⁵²M. Nooijen and R. J. Bartlett, J. Chem. Phys. **106**, 6441 (1997).
- ⁵³M. Nooijen and R. J. Bartlett, J. Chem. Phys. **106**, 6449 (1997).
- ⁵⁴M. Nooijen and R. J. Bartlett, J. Chem. Phys. **107**, 6812 (1997).
- ⁵⁵J. Sous, P. Goel, and M. Nooijen, Mol. Phys. **112**, 616638 (2014).
- ⁵⁶J. D. Watts and R. J. Bartlett, Chem. Phys. Lett. **258**, 581588 (1996).